Jurnal Teknologi

Full paper

Influence of Zinc on the Structure and Morphology of Manganese Ferrite Nanoparticles

Sahira Hassan Kareem[a], Yee Khai Ooi[a], Sabah Saeed Abdulnoor[b], Mustaffa Shamsuddin[c], Siew Ling Lee[c*]

[a]*Department of Chemistry, Faculty of Science, Universiti Teknologi Malaysia, 81310 UTM Johor Bahru, Johor, Malaysia*
[b]*Department of Physics, Faculty of Science, University Tachnology Baghdad, Iraq*
[c]*Ibnu Sina Institute for Fundamental Science Studies, Universiti Teknologi Malaysia, 81310 UTM Johor Bahru, Johor, Malaysia*

*Corresponding author: sllee@ibnusina.utm.my

Article history

Received :5 March 2014
Received in revised form :
19 April 2014
Accepted :3 May 2014

Graphical abstract

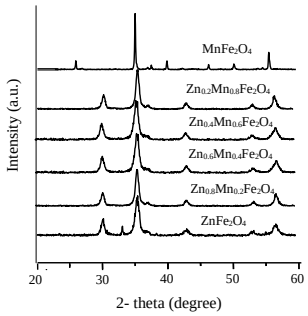

Abstract

Nanocrystalline spinel ferrites with general formula of $Mn_xZn_{1-x}Fe_2O_4$; x = 1.0, 0.8, 0.6, 0.4, 0.2, 0.1 were prepared via co-precipitation method at 75 °C and pH 11. The XRD results showed that the doping of Zn ions into ferrite's structure resulted in the reduction of both crystallinity and crystallite size. The results also revealed that the synthesized $Mn_xZn_{1-x}Fe_2O_4$ crystalline in spinel cubic structure with particle size range of 13.0 – 22.5 nm. Field emission scanning electron microscopy (FESEM) images showed an increase in particle size with the decreasing Zn content. The types of chemical covalent bonds which existed in the samples were determined via Fourier transforms infrared (FTIR) spectroscopy.

Keywords: Ferrites; chemical co-precipitation; nanostructures; X-ray diffraction

Abstrak

Ferit spinel nanokristal dengan formula am $Mn_xZn_{1-x}Fe_2O_4$; x = 1.0, 0.8, 0.6, 0.4, 0.2, 0.1 telah disediakan melalui kaedah pemendakan bersama pada 75°C dan pH 11. Analisis XRD menunjukkan bahawa pendopan ion Zn ke dalam struktur ferit mengurangkan darjah penghabluran dan saiz kristal. Kajian ini juga mendapati bahawa $Mn_xZn_{1-x}Fe_2O_4$ telah menghasilkan hablur dalam struktur kubik spinel dengan saiz zarah di antara 13.0 - 22.5 nm. Imej mikroskopi imbasan electron pemancaran medan (FESEM) telah menunjukkan peningkatan dalam saiz zarah dengan penurunan kepekatan Mn. Jenis-jenis ikatan kovalen kimia yang wujud di dalam sampel telah dikenalpasti melalui spektroskopi infra-merah transformasi Fourier (FTIR).

Kata kunci: Ferit; kimia pemendakan bersama; struktur nano; pembelauan sinar-X

1.0 INTRODUCTION

In recent years, spinel ferrites nanoparticles of $Mn_xZn_{1-x}Fe_2O_4$ have attracted considerable interest due to their widespread fundamental and technological importance [1]. These materials are versatile for various technological applications including magnetic recording, biomedicine, targeted drug delivery, magnetic fluids, data storage, spin- tonics, solar cells, sensors and catalysis [2]. They can also be employed for pharmaceutical and biomedical purposes, as well as in electronic applications. In fact, magnetic nanoparticles have been widely used in the synthesis of magnetic ferrofluid and utilized as biologically active molecules. It was reported that Mn-Zn ferrites are potential candidates as transfer devices and they can be used in drug delivery system and medical diagnostics especially in cancer treatments [3-4].

Mn and Zn modified ferrites have unique physical and chemical properties such high magnetic permeability and low core loss; the high-permeability low-power losses optical, magnetic, thermal and mechanical properties [5-6]. The physical and chemical properties of magnetic ferrite nanoparticles largely depend on the synthesis method and preparation conditions. Therefore, several techniques have been developed to synthesize nanoparticles of Zn–Mn ferrite, such as high-energy ball milling [7-8], co-precipitation [9], sol–gel [10], hydrothermal synthesis method [11] and micro emulsion technique [12]. The co-precipitation method appears to be the most promising method due to its simplicity and high productivity. This method is also able to produce products with narrow size distribution, small particle sizes and controllable shape. In fact, this method has been widely used for biomedical applications due to the ease of implementation [13-14]. The different properties of spinel structure are controlled by the cation distribution between the tetrahedral A-site and octahedral B-site. The cation distribution depends on the ionic radii of the cation, preparation method, condition for preparation, chemical composition, sintering temperature, doping and substitution process [5].

The spinel ferrite has a general formula, AB_2O_4. These ferrites, possessing the cubic spinel structure, are described with the formula of AB_2O_4, where; A and B refer to the tetrahedral and octahedral cation sites, respectively. The types of cations and their distribution between the two interstitial sites in the ferrites, determine many of the intrinsic magnetic properties of the ferrites [6-8]. Zinc ferrite, $ZnFe_2O_4$ is a normal spinel structure, where Zn^{2+} preferably occupies the tetrahedral sites due to its affinity for sp^3 bonding with oxygen anions, leaving all the ferric ions on the octahedral sites. The normal spinel structure, $ZnFe_2O_4$, is paramagnetic at room temperature due to super weak exchange interaction which could be attributed to right angle in Fe^{3+}–O–Fe^{3+} [15]. On the other hand, $MnFe_2O_4$ has partially inverse spinel structure consisting of manganese and ferric ions occupying both tetrahedral (A) and octahedral (B) sites. It has been reported that $Mn_xZn_{1-x}Fe_2O_4$ possessed a mixed spinel structure as cations Me^{2+} and Fe^{3+} occupied both A and B-positions [16-18]. The magnetic and electronic properties of these ferrites are dependent of their chemical composition, preparation method, grain size and distribution of cations between the two interstitial sites [14].

In this study, Mn-Zn ferrite nanoparticles were synthesized via co-precipitation technique. Metallic chlorides of Mn and Fe were used as the precursors in the synthesis procedure. The effect of zinc concentration on the physical and morphological properties on the Mn ferrites was also investigated.

2.0 EXPERIMENT

A series of $Mn_xZn_{1-x}Fe_2O_4$; x = 1.0, 0.8, 0.6, 0.4, 0.2, 0.1 were prepared via co-precipitation method. The chemical reagents used were ferric chloride ($FeCl_3$), manganese(II) chloride ($MnCl_2,4H_2O$), zinc chloride ($ZnCl_2$) and sodium hydroxide (NaOH). Appropriate amount of the metal chlorides were dissolved in water. The mixture solution was stirred in a reactor for 10 minutes; followed by steady addition of sodium hydroxide solution (1 M). The mixture was stirred at pH 11 at 75 °C for 1 hour. The resulting black precipitate was filtered and washed with distilled water then dried in an oven at 70 °C for 1 hour. The resulted powder was calcined at 700 °C.

The synthesized samples were characterized by X-ray diffraction (XRD using an X-ray diffractometer with high-intensity CuK_a radiation (l = 1.5418 Å).The XRD patterns were recorded at a scanning rate of 0.05 $^o s^{-1}$ with the 2θ range of 20 to 60º. Fourier transformed infrared (FTIR) spectra were taken using Perkin Elmer 5DX FTIR after mixing 1 mg of ferrite sample with 100 mg of potassium bromide (KBr). Meanwhile, scanning electron microscopy (FESEM) images were taken with a FE-SEM JSM-671F.

3.0 RESULTS AND DISCUSSION

The XRD spectra of all the synthesized samples are shown in Figure 1. The results depicted that $MnFe_2O_4$ is crystalline with inversed spinel structure in cubic phase and *Fd3m* space group (JCPDS card No. 75-0034) [19]. Meanwhile, $ZnFe_2O_4$ crystallined in normal spinel structure [20]. Obviously, the introduction of Zn into $MnFe_2O_4$ has caused the changes in crystal structure from inverse spinel structure to normal spinel structure. The Zn doped $MnFe_2O_4$ samples were crystallined in mixed spinel structure. Solid solution was formed for those Zn doped $MnFe_2O_4$ samples. Besides that, the crystallinity of the materials dropped after the addition of Zn.

The crystallite size of $Mn_xZn_{1-x}Fe_2O_4$ was calculated based on Scherrer equation.

$$D = d\lambda/(\beta \cos \theta)$$

where D is the average crystallite size of the phase under investigation, d is the Scherrer constant (0.89), λ= (1.5418 Å) is the wave length of X-ray beam used and β is the full-with half maximum (FWHM) of broadening and θ is the angle of diffraction. The crystallite size was measured by Scherrer's formula using half width of the prominent peak of maximum intensity (311) plane. The results shown in Table 1 depicts that the crystalline size of all the samples was in the range of 12.95 – 22.50 nm. Crystalline size of $MnFe_2O_4$ (22.50 nm) decreased linearly with increasing amount of Zn content. The decrease can be explained by the substitution of Mn^{2+} (0.83 Å) with Zn^{2+} (0.74 Å), which has smaller ionic radii [21]. Similarly, the reduction in both lattice parameter *a* and volume of the synthesized $Mn_xZn_{1-x}Fe_2O_4$ were observed when the amount of Zn increased in the sample.

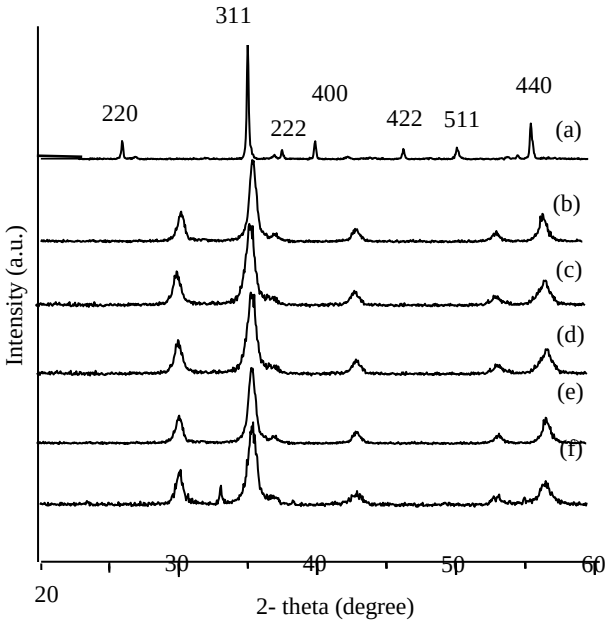

Figure 1 The XRD patterns of (a) $MnFe_2O_4$, (b) $Mn_{0.8}Zn_{0.2}Fe_2O_4$, (c) $Mn_{0.6}Zn_{0.4}Fe_2O_4$,(d) $Mn_{0.4}Zn_{0.6}Fe_2O_4$, (e) $Mn_{0.2}Zn_{0.8}Fe_2O_4$ and (f) $ZnFe_2O_4$

Figure 2 shows the FESEM images of the $Mn_xZn_{1-x}Fe_2O_4$ samples. As can be seen, the shape of the particles was in a disordered array. Besides that, agglomeration that was observed in the all samples could be due to magnetic properties of the compounds. Analysis will be carried out to determine the magnetic properties of the materials to confirm the statement. Obviously, variation in Zn amount did not give significant effect to the morphology of the samples. The particle size ranged from 20-39 nm, confirming the formation of $Mn_xZn_{1-x}Fe_2O_4$ nanoparticles. The particle size obtained was in good agreement with those calculated using Scherrer's equation (Table 1).

Table 1 The crystalline size, lattices parameter and volume of $Mn_xZn_{1-x}Fe_2O_4$ at calcination temperature of 700°C.

Sample	Crystalline size (nm)	lattice parameter *a*(Å)	Volume (cm^3)
$MnFe_2O_4$	22.50	8.541	623.27
$Mn_{0.8}Zn_{0.2}Fe_2O_4$	19.24	8.496	613.26
$Mn_{0.6}Zn_{0.4}Fe_2O_4$	18.30	8.452	603.78
$Mn_{0.4}Zn_{0.6}Fe_2O_4$	18.37	8.458	605.28
$Mn_{0.2}Zn_{0.8}Fe_2O_4$	13.60	8.424	598.01
$ZnFe_2O_4$	12.95	8.421	597.37
$Mn_{0.4}Zn_{0.6}Fe_2O_4$	18.37	8.458	605.28
$Mn_{0.2}Zn_{0.8}Fe_2O_4$	13.60	8.424	598.01
$ZnFe_2O_4$	12.95	8.421	597.37

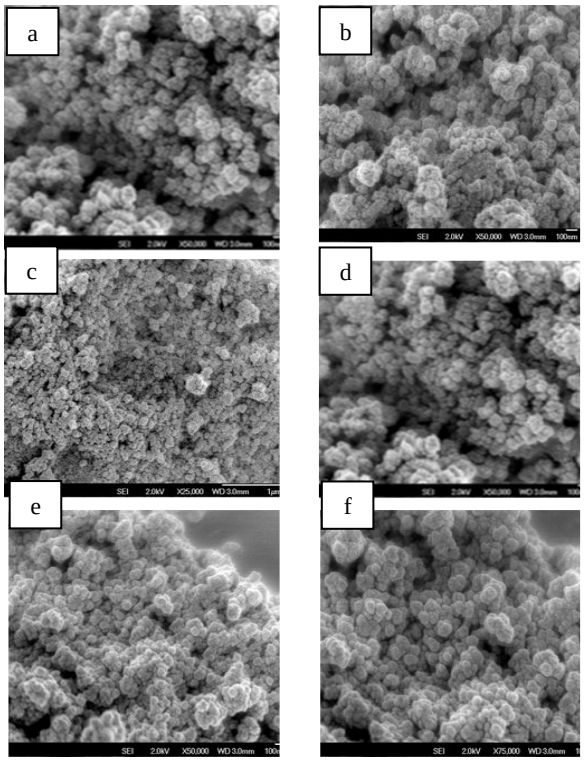

Figure 2 FESEM images for (a) $MnFe_2O_4$, (b) $Mn_{0.8}Zn_{0.2}Fe_2O_4$,(c) $Mn_{0.6}Zn_{0.4}Fe_2O_4$, (d) $Mn_{0.4}Zn_{0.6}Fe_2O_4$ (e) $Mn_{0.2}Zn_{0.8}Fe_2O_4$and (f) $ZnFe_2O_4$

FTIR spectra of the synthesized $Mn_xZn_{1-x}Fe_2O_4$ nanoparticles are illustrated in Figure 3. The spectra show characteristic peaks of magnetite powder: metal-oxygen band observed at ~590 cm^{-1} that corresponds to intrinsic stretching vibrations of the metal at tetrahedral site (M_{tetra}-----O), whereas metal-oxygen band observed at 445 cm^{-1} is assigned to octahedral-metal stretching (M_{octa}------O) [19, 22]. The differentiation in these two peaks refers to the formation of different spinel structures: normal spinel structure for $ZnFe_2O_4$; inverse spinel for $MnFe_2O_4$ and mixed spinel structure for Zn doped $MnFe_2O_4$ samples. It can also be observed that the bending and stretching modes of O–H hydroxyl groups at 1397 and 3504 cm^{-1}, respectively, exist in all of the samples, even after calcinations. As observed, these adsorption peaks were more intense in Zn-doped samples as compared to $MnFe_2O_4$. The results may imply that the introduction of Zn has increased the hydrophilicity of the Mn ferrite.

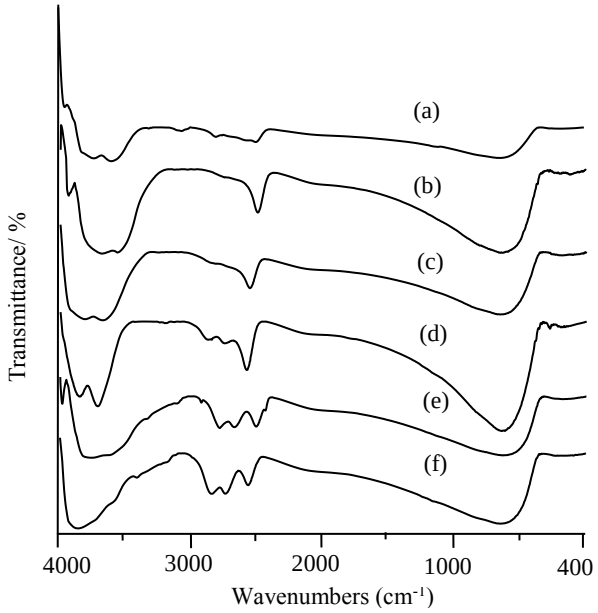

Figure 3 FTIR spectra of (a) $MnFe_2O_4$, (b) $Mn_{0.8}Zn_{0.2}Fe_2O_4$, (c) $Mn_{0.6}Zn_{0.4}Fe_2O_4$, (d) $Mn_{0.4}Zn_{0.6}Fe_2O_4$, (e) $Mn_{0.2}Zn_{0.8}Fe_2O_4$ and (f) $ZnFe_2O_4$

4.0 CONCLUSION

A series of $Mn_xZn_{1-x}Fe_2O_4$ nanoparticles have been successfully synthesized via co-precipitation method. Results showed that the Zn doping into $MnFe_2O_4$ has caused changes in the crystal structure from inverse spinel structure to normal spinel structure. Besides that, the crystallinity and crystalline size of the samples decreased from 22.50 to 12.95 nm, upon the introduction of Zn. Due to the smaller ionic radii of Zn^{2+}, reduction in both lattice parameter a and volume of the crystal was observed. However, Zn did not have any significant effect on the morphology of the resulted samples. The presence of Zn has affected the type of metal-oxygen band formed in the samples.

Acknowledgement

The authors thank the Ministry of Higher Education (MOHE) through Research University Grant Scheme (Vote No. QJ130000.2526.03H90) for the financial support. The authors also thank Universiti Teknologi Malaysia (UTM), Malaysia for characterization facilities and Prof. Dr. Hadi Nur for the fruitful discussion.

References

[1] N. M. Deraz. 2012. *Ceram. Int*. 38(1): 511–516.
[2] M. Kooti, M. Afshari. 2012. *Mater. Res. Bull.* 47(11): 3473–3478.
[3] R. J. Joseyphus, A. Narayanasamy, K. Shinoda, B. Jeyadevan, K. Tohji. 2006. *J. Chem. Solids*. 67(7): 1510–1517.
[4] A. C. F. M. Costa, E. Tortella, M. R. Morelli, R. H. G. A. Kiminami. 2003. *J. Magn. Magn. Mater*. 256(1): 174–182.
[5] N. M. Deraz, A. Alarifi. 2012. *Int. J. Electrochem. Sci*. 7(7): 6501–6511.
[6] J. Wang, C. Zeng, Z. Peng, Q. Chen. 2004. *Physica B.* 349(1): 124–128.
[7] R. V. Mangalaraja, S. Ananthakmar, P. Manohar, F. D. Gnanam, M. Awano. 2004. *Mater. Sci. Eng. A.* 367: 301–305.
[8] W. H. Lin., S. K. J. Jean, C. S. Hwang. 1999. *J. Mater. Res.* 14(01): 204–208.
[9] S. K. Pradhan, S. Bid, M. Gateshki, V. Petkov. 2005. *Mater. Chem. Phys.* 93(1): 224–230.
[10] R. Arulmurugan, B. Jeyadevan, G. Vaidyanathan, S. Sendhilnatha. 2005. *J. Magn. Magn. Mater*. 288: 470–477.
[11] A. Thakur, P. Mathur, M. Singh. 2007. *J. Phys. Chem. Solids*. 68(3): 378–381.
[12] Z. G. Zheng, X. C. Zhong, Y. H. Zhang, H. Y. Yu, D. C. Zeng. 2008. *J. Alloy. Compd.* 466(1): 377–382.
[13] K. Verma, R. Rai, S. Sharma. 2010. *Integr. Ferroelectr*. 119(1): 55–65.
[14] S. Amiri, H. Shokrollahi. 2013. *Mater. Sci. Eng. C.* 33(1): 1–8.
[15] H. Shokrollahi. 2013. *Mater. Sci. Eng. C*. 33: 2476–2487.
[16] N. M. Deraz, A. Alarifi. 2009. *Polyhedron*. 28(18): 4122–4130.
[17] R. Iyer, R. Desai, R.V. Upadhyay. 2009. *B. Mater. Sci.* 32(2): 141–147.
[18] D. S. Mathew, R. S. Juang. 2007. *Chem. Eng. J*. 129(1): 51–65.
[19] S. R. Kulal, S. S. Khetre, P. N. Jagdale, V. M. Gurame, D. P. Waghmode, G. B. Kolekar, S. R Sabale, S. R. Bamane. 2012. *Mater. Lett.* 84: 169–172.
[20] Q. Li, C. Bo, W. Wang. 2010. *Mater. Chem. Phys*. 124(2): 891–893.
[21] R. D. Shannon. 1976. *Acta Cryst.* A. 32: 751
[21] A. A. Ati, Z. Othaman, A. Samavati. 2013. *J. Mol. Struct.* 1052: 177–182.